

Chapter 20

The resistive tearing instability*

In the previous Chapter, we analyzed an important instability, the Rayleigh–Taylor (or flute) instability, which can arise in an ideal magnetohydrodynamic (MHD) plasma, i.e. a plasma in which the electrical resistivity is assumed to be zero and where the additional terms that enter in the ‘generalized’ Ohm’s law are also negligible. For such cases, as we have seen, the plasma and the magnetic field are ‘frozen’ together. We found the flute instability to be very rapidly growing, with a growth time comparable to the time it takes a sound wave to travel a distance that is the geometric mean of the size of the plasma and the radius-of-curvature of the magnetic field. Since sound waves travel rapidly in high-temperature plasmas, such times are very short.

Even if a plasma is not subject to MHD instabilities, to be certain that it is *completely* stable we must also examine non-MHD perturbations that have the potential to grow at much slower rates. We have seen that the ideal MHD approximation breaks down for very long time-scales: eventually, the plasma will ‘leak’ across the magnetic field or, equivalently, the magnetic field will ‘diffuse’ into the plasma. Thus for slow plasma phenomena, non-zero resistivity must be included in the stability analysis, specifically in the plasma Ohm’s law. Although resistivity often acts to damp out perturbations, there are important cases where resistivity is actually *destabilizing*. Indeed, there is an entirely new class of plasma instabilities, of which the most important is the ‘resistive tearing instability’ to be discussed here, that arise only in the presence of resistivity. The reason why resistivity can be destabilizing is that it frees the plasma from the constraint that it remain ‘frozen’ to the magnetic field, thereby allowing qualitatively different types of plasma perturbations. In particular, these ‘resistive’ perturbations can more effectively draw upon the magnetic energy generated by currents in the plasma itself, which is available to drive instabilities.

Intuitively, one might expect that ‘resistive instabilities’ would grow

exceedingly slowly, specifically on time-scales comparable to the characteristic times for resistive diffusion of plasma across a magnetic field. If so, they would be of little interest, since most plasma equilibria are changing on such time-scales anyway, and the occurrence of a comparably slowly growing mode of instability might not make much difference in practice. However, some resistive instabilities, certainly including the tearing instabilities to be considered here, *grow much faster than this*. The reason is that the instability is able to take whatever form most efficiently releases the magnetic energy on which it feeds. Just as the flute instability was found to be driven by the non-uniformity of the plasma *pressure* (i.e. by the plasma *thermal* energy), the resistive tearing instability in its simplest form is driven by various types of non-uniformity of the *magnetic field* (i.e. by the ability of the *magnetic* energy to find a path to a lower energy state). It is this 'pent up' energy in the magnetic field, trying to find a way to relax to a lower energy state, that drives the tearing instability. The growth rate can be larger than one might intuitively expect because the resistive diffusion of plasma across the magnetic field occurs on a much shorter spatial scale-length than the plasma size and yet still can release significant amounts of magnetic energy; because of the shorter scale-length, the resistive diffusion can proceed quite quickly. The theory of resistive tearing instabilities, including their surprisingly large growth rates, was developed first in a paper by H P Furth, J Killeen and M N Rosenbluth (1963 *Phys. Fluids* 6 459).

20.1 THE PLASMA CURRENT SLAB

We will analyze the resistive tearing instability for the simplest configuration in which it occurs, namely a 'plasma current slab'. Specifically, we consider an infinite plasma that contains a finite slab (or thick sheet) of current, directed parallel to the surface of the slab, namely

$$j_z = \begin{cases} j_{z0} & -a < x < a \\ 0 & |x| > a. \end{cases} \quad (20.1)$$

The plasma is uniform in the y and z directions. Solving Ampere's law, $\nabla \times \mathbf{B} = \mu_0 \mathbf{j}$, i.e. $dB_y/dx = \mu_0 j_z(x)$, we obtain

$$B_y(x) = \begin{cases} B'_{y0}x & -a < x < a \\ -B'_{y0}a & x < -a \\ B'_{y0}a & x > a \end{cases} \quad (20.2)$$

where $B'_{y0} = \mu_0 j_{z0}$. The functions $j_z(x)$ and $B_y(x)$ are sketched in Figure 20.1.

The magnetic field lines in the (x, y) plane are illustrated in Figure 20.2. Here, we have indicated the strength of the B_y field at different locations x by the density of field lines at x : the field is stronger where the field lines are

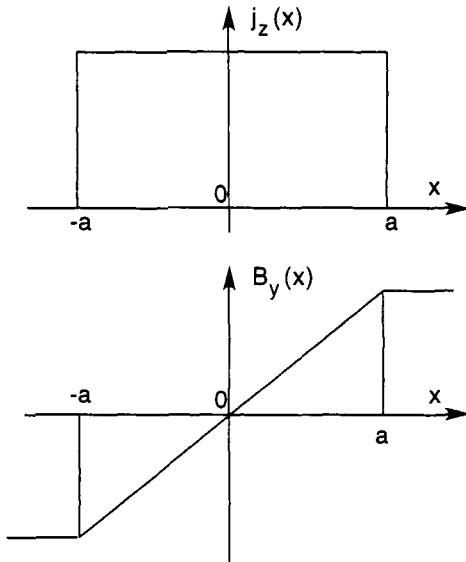


Figure 20.1. The 'plasma current sheet' equilibrium.

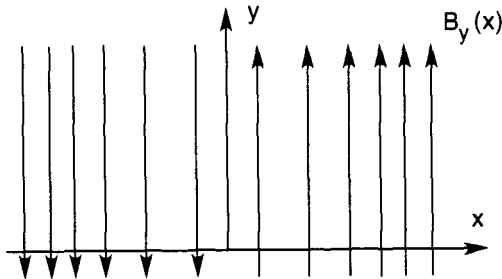


Figure 20.2. Magnetic field lines for the 'plasma current sheet' equilibrium. There is also a strong approximately uniform field B_z .

more crowded together. This plasma could possibly be subject to ideal MHD perturbations (although we will in fact find it to be ideal-MHD stable), but these would not change the basic configuration, since the magnetic flux through any plasma surface element in the (x, z) plane (i.e. the number of magnetic field lines of the B_y field crossing such a surface element) must remain fixed. However, the inclusion of plasma resistivity will allow the negative B_y field on the left of $x = 0$ to diffuse into the region of positive B_y field on the right of $x = 0$, thereby *annihilating* it. This 'annihilation' (or 'cancelling out') of the magnetic field will clearly occur most effectively in the vicinity of $x = 0$, which is where

we will find the largest plasma flows in the resistive tearing instability.

It is easy to see that this annihilation of magnetic field is *energetically favored*. For example, if we consider the modification of $B_y(x)$ that would result from cancellation of the positive and negative B_y components in some small region $|x| < \delta$, it is clear that the magnetic energy, $\int (B_y^2/2) dV$, would be reduced. The actual resistive tearing instability cannot annihilate magnetic field in such a neat and simple way: rather it involves wave-like perturbations of the entire plasma, well to the left and right of $x = 0$, which cause a wave-like 'break-up' of the magnetic topology near $x = 0$. Overall, however, the magnetic energy is lowered by this type of perturbation.

The current-slab configuration illustrated in Figure 20.2 may have an additional magnetic field in the z direction. If such a field is *not* present, the plasma can be in equilibrium only if it has a pressure $p(x)$ that varies in x in such a way as to balance the variation in magnetic pressure, i.e. to satisfy $p + B_y^2/2\mu_0 = \text{constant}$. On the other hand, if a *large* B_z field is introduced, small variations of it will easily be sufficient to balance the pressure variations (assuming $p \ll B_z^2/2\mu_0$), and the functions $p(x)$ and $B_y(x)$ become essentially independent of each other. A strong B_z field will also play another role: as in the case of the Rayleigh–Taylor instability, it will constrain the plasma flow in the (x, y) plane to be incompressible, satisfying $\nabla \cdot \mathbf{u}_\perp = 0$. In the particular example analyzed in this Chapter, we will assume that a strong B_z field *is* in fact present. It should be emphasized that these assumptions are made largely for analytic simplicity. Resistive tearing instabilities can occur at a surface where $B_y(x) = 0$, if energetically favored, even with finite pressure in the equilibrium and a weak (or zero) B_z field, so that the flow becomes compressible.

Once the B_z field is introduced, it becomes clear that the configuration we are considering is simply one particular example of more general 'plane slab' configurations with field components $B_y(x)$ and $B_z(x)$. Due to the variation of B_y and/or B_z with x , the direction of the magnetic-field vector rotates as we move in the x direction. Such fields are said to be 'sheared'. For sheared fields, the directions of the y and z axes can be chosen so that the field points exactly in the z direction at some selected point, say $x = 0$. The configuration then looks exactly like the one illustrated in Figures 20.1 and 20.2 (with a B_z field added). Thus, in regard to tearing instabilities, our particular example is, in fact, representative of a wider class of sheared-field configurations.

Since these plane slab equilibria are stationary in time and uniform in the y and z directions, linearized perturbations of the equilibria may be Fourier analyzed into normal modes of the form

$$\psi_1(\mathbf{x}, t) = \hat{\psi}_1(x) \exp(ik_y y + ik_z z - i\omega t)$$

where $\psi_1(\mathbf{x}, t)$ is any first-order perturbation quantity. For the particular equilibrium defined by equations (20.1) and (20.2), which has $B_y(x) = 0$ on

the surface $x = 0$, the resistive tearing instabilities have $k_z = 0$, i.e. the \mathbf{k} -vector is exactly perpendicular to \mathbf{B} at $x = 0$, i.e. $\mathbf{k} \cdot \mathbf{B} = 0$ at the location of the tearing instability. When a B_z field is introduced, so that we have a sheared-field configuration with both $B_y(x)$ and $B_z(x)$, it is clear that all surfaces $x = \text{constant}$ are potential locations for tearing instabilities, for we can orient the y and z axes so that the magnetic field lies in the z direction on any particular surface, and we can then choose a \mathbf{k} -vector in the y direction, subject of course to this being allowed by the boundary conditions. For a plane slab that extends infinitely far in the y and z directions, all k_y and k_z values are allowed: for a slab of finite extent, the allowed values are determined by the boundary conditions, which will then generally limit the surfaces on which tearing instabilities may be located. For the present analysis, we will limit ourselves to the equilibrium of equations (20.1) and (20.2) and perturbations with k_y only, i.e. $k_z = 0$. This simply puts the 'resonant surface' where $\mathbf{k} \cdot \mathbf{B} = 0$ at the location $x = 0$. At this resonant surface, a zeroth-order magnetic field line lies along a line of constant phase in the wave-like perturbation, making it very susceptible to the first-order magnetic perturbation. We will further simplify the notation by dropping the suffix 'y' from k_y , since this is the only non-zero component of the \mathbf{k} -vector. Thus, for the remainder of this Chapter, the perturbations are assumed to vary as $\exp(iky)$.

20.2 IDEAL MHD STABILITY OF THE CURRENT SLAB

As we saw in our treatment of the Rayleigh–Taylor instability in Chapter 19, some general properties of the magnetic field perturbations can be obtained from the linearized version of the combination of Faraday's law and Ohm's law. First, we consider a perfectly conducting plasma, in which case we obtain

$$\begin{aligned} \frac{\partial \mathbf{B}_1}{\partial t} &= -\nabla \times \mathbf{E}_1 = \nabla \times (\mathbf{u}_1 \times \mathbf{B}_0) \\ &= (\mathbf{B}_0 \cdot \nabla) \mathbf{u}_1 - (\mathbf{u}_1 \cdot \nabla) \mathbf{B}_0 - \mathbf{B}_0 (\nabla \cdot \mathbf{u}_1) \end{aligned} \quad (20.3)$$

noting that the plasma velocity \mathbf{u} is zero in the equilibrium and has only a perturbed value, denoted by \mathbf{u}_1 . Unlike the geometry for the Rayleigh–Taylor instability, in the case considered here the field lines become *bent*, i.e. both a first-order B_x component and a first-order perturbed B_y component arise. Accordingly, the x and y components of equation (20.3) provide some non-trivial information, namely

$$\frac{\partial B_{x1}}{\partial t} = ik B_{y0} u_{x1} \quad (20.4)$$

and

$$\begin{aligned}
 \frac{\partial B_{y1}}{\partial t} &= ikB_{y0}u_{y1} - u_{x1} \frac{\partial B_{y0}}{\partial x} - B_{y0}(\nabla \cdot \mathbf{u}_1) \\
 &= -u_{x1} \frac{\partial B_{y0}}{\partial x} - B_{y0} \frac{\partial u_{x1}}{\partial x} \\
 &= -\frac{\partial}{\partial x}(B_{y0}u_{x1}).
 \end{aligned} \tag{20.5}$$

(Equation (20.5) could also have been derived by combining equation (20.4) with the requirement that $\nabla \cdot \mathbf{B}_1 = 0$.) For a normal mode with frequency ω , i.e. with perturbation quantities varying as $\exp(-i\omega t)$ such as we are seeking, equation (20.4) can be written simply

$$\omega B_x = -k B_{y0} u_x \tag{20.6}$$

in which, here and henceforth, we drop the suffix '1' from the velocity and field components u_x and B_x , respectively, since these components are zero in the equilibrium. We note, in passing, that equation (20.6) requires that B_x vanish at any point where $B_{y0} = 0$, in particular at $x = 0$ in our example: otherwise, the velocity component u_x would be infinite.

Let us now turn to the linearized first-order perturbed equation of motion, namely

$$\begin{aligned}
 \rho_0 \frac{\partial \mathbf{u}_1}{\partial t} &= -\nabla p_1 + (\mathbf{j} \times \mathbf{B})_1 \\
 &= -\nabla \left(p_1 + \frac{\mathbf{B}_0 \cdot \mathbf{B}_1}{\mu_0} \right) + \frac{1}{\mu_0} [(\mathbf{B}_0 \cdot \nabla) \mathbf{B}_1 + (\mathbf{B}_1 \cdot \nabla) \mathbf{B}_0].
 \end{aligned} \tag{20.7}$$

We have used $\mathbf{j} = (\nabla \times \mathbf{B})/\mu_0$ and the vector identity for $(\nabla \times \mathbf{B}) \times \mathbf{B}$ (see Appendix D). We have also linearized the magnetic pressure perturbation, writing $(B^2)_1 = 2\mathbf{B}_0 \cdot \mathbf{B}_1$. Both x and y components of this linearized equation of motion provide useful information, namely

$$-i\omega\rho_0 u_x = -\frac{\partial}{\partial x} \left(p_1 + \frac{B_{z0}B_{z1} + B_{y0}B_{y1}}{\mu_0} \right) + \frac{1}{\mu_0} ikB_{y0}B_x \tag{20.8}$$

$$-i\omega\rho_0 u_y = -ik \left(p_1 + \frac{B_{z0}B_{z1} + B_{y0}B_{y1}}{\mu_0} \right) - \frac{1}{\mu_0} \left(B_{y0} \frac{\partial B_x}{\partial x} - B_x \frac{\partial B_{y0}}{\partial x} \right). \tag{20.9}$$

In the second-to-last term on the right-hand side in equation (20.9), we have used $\nabla \cdot \mathbf{B}_1 = 0$ to express B_{y1} in terms of B_x . Just as in our treatment of the Rayleigh–Taylor instability we take note of the fact that, beyond equations (20.8) and (20.9) themselves, we do not have any additional information on either

p_1 or B_{z1} . In principle, we could obtain p_1 , for example from an adiabatic equation of state. Normally, we would obtain B_{z1} from the z component of equation (20.3), but this will involve the compressible, i.e. non-divergence-free, part of the plasma fluid velocity, which we expect to be very small. In the approximately incompressible case, B_{z1} is determined from either equation (20.8) or equation (20.9); when the value so determined is substituted into the z component of equation (20.3), this will yield a value for the compressible part of the fluid velocity, i.e. for $\nabla \cdot \mathbf{u}_1$, but this is a small quantity that does not enter anywhere else. Physically, the very small B_{z1} produces whatever modification of the almost-uniform magnetic pressure B_z^2 is needed to maintain force balance against small changes in pressure, in approximately incompressible flow. Both the Rayleigh–Taylor (gravitational) instability and the tearing instability are thus essentially independent of plasma pressure. The Rayleigh–Taylor instability is driven by the energy available from the inverted density gradient (relative to the gravitational force), and the tearing instability can be driven purely by the energy available from the sheared magnetic field. We will see, however, that this magnetic energy will become available to the plasma motion only through resistivity.

Just as we did in the case of the Rayleigh–Taylor instability, we can eliminate the two quantities p_1 and B_{z1} by forming the z component of the curl of the equation of motion. Specifically, we take $\partial/\partial x$ of the y component, equation (20.9), and subtract ik times the x component, equation (20.8). This produces

$$\begin{aligned} -i\omega \left(\frac{\partial}{\partial x} (\rho_0 u_y) - ik\rho_0 u_x \right) &= \frac{1}{\mu_0} \left[\frac{\partial}{\partial x} \left(B_x \frac{\partial B_{y0}}{\partial x} - B_{y0} \frac{\partial B_x}{\partial x} \right) + k^2 B_{y0} B_x \right] \\ &= -\frac{1}{\mu_0} \left\{ \frac{\partial}{\partial x} \left[B_{y0}^2 \frac{\partial}{\partial x} \left(\frac{B_x}{B_{y0}} \right) \right] - k^2 B_{y0} B_x \right\}. \end{aligned} \quad (20.10)$$

At this point, our analysis is still valid for a general equilibrium $B_{y0}(x)$ and is not limited to the equilibrium defined by equation (20.2).

Let us, for the moment, suppose that the plasma motion is exactly incompressible, i.e.

$$0 = \nabla \cdot \mathbf{u}_1 = \frac{\partial u_x}{\partial x} + ik u_y. \quad (20.11)$$

As in the case of the Rayleigh–Taylor instability, this assumption is only approximately valid. Its validity could be verified after we have completed our calculation, in exactly the same way as was done in Chapter 19. Specifically, we could relate $\nabla \cdot \mathbf{u}_1$ to the perturbation B_{z1} produced by compressing the strong magnetic field B_{z0} (see equation (19.20)). We could then relate the force arising from the gradient of the perturbed magnetic pressure $B_{z0} B_{z1}$ to either u_x

or u_y (see, for example, equation (19.22)). Comparing the magnitude of $\nabla \cdot \mathbf{u}_1$ with either of its constituent terms (in this case, $\partial u_x / \partial x$ or iku_y), we would find that $\nabla \cdot \mathbf{u}_1$ is smaller by a factor $\omega^2 / k^2 v_A^2$, where v_A is the Alfvén speed, $B_0 / (\rho_0 \mu_0)^{1/2}$. As in the case of the Rayleigh–Taylor instability, the frequencies (or growth rates) of even the fastest modes that will be found here are much less than kv_A . Hence, again, the compressibility is negligible, and we may to a very good approximation write $\nabla \cdot \mathbf{u}_1 = 0$.

Using equation (20.11) to substitute for u_y in terms of u_x , the left-hand side of equation (20.10) can be expressed entirely in terms of u_x , so that this equation becomes

$$-\frac{\omega \mu_0}{k} \left[\frac{\partial}{\partial x} \left(\rho_0 \frac{\partial u_x}{\partial x} \right) - k^2 \rho_0 u_x \right] = \frac{\partial}{\partial x} \left[B_{y0}^2 \frac{\partial}{\partial x} \left(\frac{B_x}{B_{y0}} \right) \right] - k^2 B_{y0} B_x. \quad (20.12)$$

For perfect conductivity, equation (20.6) is valid and can now be used in the form

$$B_x / B_{y0} = -ku_x / \omega \quad (20.13)$$

to express the right-hand side of equation (20.12) also in terms of u_x . Multiplying through by $-\omega k$ and rearranging terms slightly, equation (20.12) can now be written

$$\frac{\partial}{\partial x} \left((\rho_0 \mu_0 \omega^2 - k^2 B_{y0}^2) \frac{\partial u_x}{\partial x} \right) - k^2 (\rho_0 \mu_0 \omega^2 - k^2 B_{y0}^2) u_x = 0. \quad (20.14)$$

Equation (20.14) is a homogeneous second-order differential equation for u_x . It describes ideal MHD waves in the configuration being considered. With proper boundary conditions, eigenmode solutions to the equation could be found. However, certain general properties of such waves can be determined by examining the quadratic (in u_x) expression formed by multiplying equation (20.14) by the complex conjugate u_x^* and integrating over all x , i.e. from $-\infty$ to $+\infty$. The result, after integrating by parts and noting that u_x must vanish as $x \rightarrow \pm\infty$, is

$$\int_{-\infty}^{\infty} (\rho_0 \mu_0 \omega^2 - k^2 B_{y0}^2) \left(\left| \frac{\partial u_x}{\partial x} \right|^2 + k^2 |u_x|^2 \right) dx = 0. \quad (20.15)$$

By examining equation (20.15), it is evident first that ω^2 must be real, so that ω must be either real or pure imaginary. It is further evident that our plasma must be completely stable (under this assumption of perfect conductivity), since an instability must correspond to a pure imaginary value of ω , i.e. $\omega = i\gamma$ for $\gamma > 0$, which would render the left-hand side of equation (20.15) negative-definite, so that it certainly could not be equal to zero.

The stable oscillatory waves that are described by equation (20.14) are the 'shear Alfvén waves' in the low-frequency limit introduced in Chapter 18. We note that their frequencies are typically $\omega \sim k_{\parallel} v_A$, where $k_{\parallel} = \mathbf{k} \cdot \hat{\mathbf{b}} = k_y B_{y0}/B_z$ is the component of the wave vector in the direction of the equilibrium magnetic field. The particular configuration under discussion here, however, has a special property, namely that B_{y0} depends on x . If the value of $\omega(\rho_0\mu_0)^{1/2}$ falls into the range of values assumed by $kB_{y0}(x)$, then equation (20.14) becomes *singular*, in that the coefficient of the second derivative can vanish. Since our main interest here is in instabilities, not stable oscillations, we need not explore this matter further. It is sufficient to note that the spectrum of possible solutions of equation (20.14) contains discrete modes with $\omega > k|B_{y0}|_{\max}/(\rho_0\mu_0)^{1/2}$ and a continuum of modes with smaller ω values that are generally subject to strong damping at the location of the singularity due to effects not included in the ideal MHD analysis.

20.3 INCLUSION OF RESISTIVITY: THE TEARING INSTABILITY

Let us now introduce resistivity into the plasma Ohm's law, i.e.

$$\mathbf{E} + \mathbf{u} \times \mathbf{B} = \eta \mathbf{j}. \quad (20.16)$$

Combining this with Faraday's law and linearizing, the magnetic field perturbation is now given by

$$\frac{\partial \mathbf{B}_1}{\partial t} = -\nabla \times \mathbf{E}_1 = \nabla \times (\mathbf{u}_1 \times \mathbf{B}_0) - \eta \nabla \times \mathbf{j}_1 \quad (20.17)$$

where we have taken the resistivity to be uniform. Invoking Ampere's law for \mathbf{j}_1 , i.e. $\mu_0 \mathbf{j}_1 = (\nabla \times \mathbf{B}_1)$, and making use of the identity $\nabla \times (\nabla \times \mathbf{B}_1) = \nabla(\nabla \cdot \mathbf{B}_1) - \nabla^2 \mathbf{B}_1 = -\nabla^2 \mathbf{B}_1$ (see Appendix D), we obtain

$$\frac{\partial \mathbf{B}_1}{\partial t} = \nabla \times (\mathbf{u}_1 \times \mathbf{B}_0) + \frac{\eta}{\mu_0} \nabla^2 \mathbf{B}_1. \quad (20.18)$$

Using the expansion of the first term on the right-hand side of equation (20.3), the x component of equation (20.18) becomes

$$\omega B_x = -k B_{y0} u_x + \frac{i\eta}{\mu_0} \frac{\partial^2 B_x}{\partial x^2}. \quad (20.19)$$

Here we have approximated $\nabla^2 \approx \partial^2/\partial x^2$ in anticipation of finding that resistivity is important only in a narrow region of x , within which B_x is relatively sharply varying. Equation (20.19) replaces equation (20.6) in the resistive case.

Several important conclusions follow from examination of equation (20.19). First, it is clear that our previous ideal MHD treatment corresponds to the case

$$\omega B_x \gg \frac{\eta}{\mu_0} \frac{\partial^2 B_x}{\partial x^2}. \quad (20.20)$$

For the shear Alfvén waves we have been studying, which generally have quite high frequencies ω compared to resistive diffusion rates, this relation is valid in all but the most resistive plasmas. However, we might legitimately inquire whether other modes of perturbation are possible, which have much lower frequencies or much shorter scale-lengths, such that the two terms in equation (20.20) are comparable.

For such modes, the resistive term in equation (20.19) must be retained. A second important conclusion now follows from equation (20.19): namely, it is no longer necessary for the first-order perturbation B_x to vanish at points where $B_{y0} = 0$, i.e. at $x = 0$ in the particular example shown in Figures 20.1 and 20.2. Physically, relaxing the constraint that $B_x = 0$ wherever $B_{y0} = 0$ allows the plasma much more freedom in finding ways to lower its magnetic energy, corresponding to more possibilities for unstable perturbations. A third conclusion that follows from examination of equation (20.19) is that the resistive term is likely to be most important in a narrow region around the point where $B_{y0} = 0$, i.e. around $x = 0$ in our particular example. We call this the 'resistive layer'. Since $\mathbf{k} \cdot \mathbf{B} = 0$ at $x = 0$, the perturbation can be considered to be 'resonant' at $x = 0$, such that the unperturbed magnetic field lies parallel to wave-fronts on this surface. The non-zero η in the resistive layer then allows the magnetic field lines to *connect across* the resonance, via a finite value of B_x .

Well away from the resistive layer, both to the left and to the right of $x = 0$ in the particular case illustrated in Figure 20.1, we expect the ideal MHD approximation to remain valid. Since the frequencies ω (or, more appropriately, the growth rates γ) are much less than Alfvén-wave frequencies, the perturbations in these ideal MHD regions will be given by equation (20.14) (or, equivalently, equation (20.12)) *but with the inertia terms omitted*. Since it is more convenient to describe the perturbations in the ideal MHD regions in terms of B_x rather than u_x , we prefer to work from equation (20.12), obtaining

$$\frac{\partial}{\partial x} \left[B_{y0}^2 \frac{\partial}{\partial x} \left(\frac{B_x}{B_{y0}} \right) \right] - k^2 B_{y0} B_x = 0. \quad (20.21)$$

This equation describes the perturbations in the 'outer-regions' well to the left and well to the right of the resistive layer around $x = 0$. As $x \rightarrow 0$ (either from the left or from the right), taking $B_y(x) \approx B'_{y0} x$, the possible forms for the solution B_x as $x \rightarrow 0$ are twofold: either $B_x \propto x$ or $B_x \approx \text{constant}$.

Problem 20.1: Prove the last statement by searching for solutions of equation (20.21) with $B_x \propto x^\beta$ as $x \rightarrow 0$. You will find that the first term on the left-hand side of equation (20.21) tends to dominate as $x \rightarrow 0$, allowing only solutions with $\beta = 0$ or $\beta = 1$. Why is it safe to assume that there are only these two solutions as $x \rightarrow 0$?

It is possible to see, however, that the case $B_x \propto x$ as $x \rightarrow 0$, is excluded for solutions that are well behaved as $x \rightarrow \pm\infty$ for, if B_x/B_{y0} were finite as $x \rightarrow 0$, it would be permissible to multiply equation (20.21) by B_x^*/B_{y0} and integrate from $x = -\infty$ to $x = 0$. If we then integrate the first term by parts, noting that $B_{y0} = 0$ at $x = 0$, we obtain

$$B_x^* B_{y0} \frac{\partial}{\partial x} \left(\frac{B_x}{B_{y0}} \right) \Big|_{-\infty}^0 - \int_{-\infty}^0 B_{y0}^2 \left| \frac{\partial}{\partial x} \left(\frac{B_x}{B_{y0}} \right) \right|^2 dx - \int_{-\infty}^0 k^2 |B_x|^2 dx = 0. \quad (20.22)$$

Since we want a localized solution in which $B_x \rightarrow 0$ as $x \rightarrow \infty$ (otherwise there would be infinite magnetic energy $|B_x|^2$, which is not a physically interesting case), the first term on the left-hand side vanishes in the $x \rightarrow -\infty$ limit. We then cannot allow $B_x \propto x$ as $x \rightarrow 0$, for this would make the first term on the left-hand side vanish in the $x \rightarrow 0$ limit also, and we would then have a negative-definite expression on the left, which is required to be zero.

Thus, we conclude that the only allowed solutions of equation (20.21) are such that B_x approaches some non-zero constant as $x \rightarrow 0$, either from the left or from the right. Such solutions would not be allowed by the ideal MHD constraint, i.e. equation (20.6), applied *exactly* at the point $x = 0$, for *this constraint requires B_x to be zero*. Such solutions *are* allowed in the resistive case, in which equation (20.19) replaces equation (20.6) in the vicinity of $x = 0$. It is just this non-vanishing of B_x at the point where $B_{y0} = 0$ that characterizes the ‘resistive tearing’ instability.

It is useful to think of the region around $x = 0$ as forming a ‘boundary layer’ between the two ideal MHD regions to the left and right of it. Moreover, it is possible to obtain some useful and revealing ‘boundary conditions’ by integrating various plasma equations over a thin box placed in this boundary layer, as illustrated in Figure 20.3. The box is supposed to have an infinitesimal width in x (but wider than the resistive layer) and a height in y that is finite but much less than the characteristic wavelength of the perturbation; its extent in z is arbitrary, since there are no variations in the z direction. Integrating the equation $\nabla \cdot \mathbf{B}_1 = 0$ over the volume of the box and applying Gauss’ theorem, we find that B_x must be continuous across the boundary, i.e.

$$B_x(x \rightarrow 0+) = B_x(x \rightarrow 0-). \quad (20.23)$$

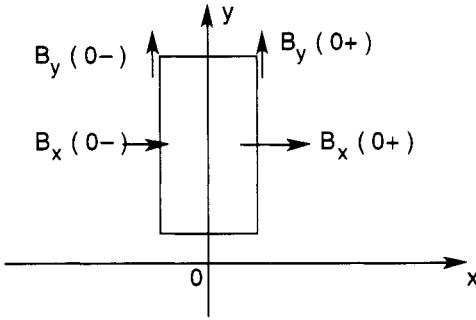


Figure 20.3. Thin box used for obtaining boundary conditions across the resistive layer.

From this we deduce that the value of B_x at each y -value may be taken to be constant throughout the resistive layer around $x = 0$. Similarly, integrating $\nabla \times \mathbf{B} = \mu_0 \mathbf{j}$ over the surface of the box in the (x, y) -plane and applying Stokes's theorem for the surface integral of a curl, we find that any discontinuity in B_{y1} must be associated with a first-order 'surface current' J_{z1} flowing in the boundary layer, i.e.

$$B_{y1}(x \rightarrow 0+) - B_{y1}(x \rightarrow 0-) = \mu_0 J_{z1}. \quad (20.24)$$

(By a 'surface current', we mean here a very large current density j_{z1} concentrated in a very narrow layer of thickness Δx , such that $J_{z1} = j_{z1} \Delta x = \text{finite}$. A highly conducting plasma has the capability to carry such currents; in the limit of resistivity decreasing toward zero, the thickness of the current layer approaches zero, and a true surface current arises.) Equation (20.24) thus indicates that the y component of the field perturbation can be discontinuous across the boundary layer. From the divergence-free property of \mathbf{B}_1 , i.e.

$$\frac{\partial B_x}{\partial x} + ik B_{y1} = 0 \quad (20.25)$$

we note that a discontinuity in B_{y1} implies a discontinuity in $\partial B_x / \partial x$. Thus, although B_x itself is continuous across the boundary layer, its gradient in x is not. Indeed, the quantity

$$\Delta' = \frac{1}{B_x} \left[\frac{\partial B_x}{\partial x} \right]_{x=0} = \frac{1}{B_x} \left(\left. \frac{\partial B_x}{\partial x} \right|_{x=0+} - \left. \frac{\partial B_x}{\partial x} \right|_{x=0-} \right) \quad (20.26)$$

where the notation $[]_{x=0}$ is seen to denote the discontinuous jump across the boundary layer at $x = 0$; this is an important quantity, which will turn out to determine the stability of resistive tearing modes.

It is clear that the 'outer-region' solutions will completely determine the quantity Δ' . We could imagine integrating equation (20.21) for B_x in the region

well to the left of $x = 0$, applying the appropriate boundary condition (usually $B_x \rightarrow 0$) at $x \rightarrow -\infty$ (or at some intervening boundary, e.g. a conducting wall). Indeed, we could carry out a numerical integration of equation (20.21), beginning at a conducting wall far to the left, where we would set $B_x = 0$ and would choose some arbitrary non-zero value for $\partial B_x/\partial x$, which simply measures the amplitude of our solution for B_x in this region. This solution will give some finite value of B_x at $x = 0$, approaching from the left, and this value provides an alternative measure of the amplitude of our solution. Thus, choosing some arbitrary value for the amplitude B_x at $x = 0$ (noting that the amplitude of a linear perturbation will always be arbitrary, within the confines of the linearized theory), the outer-region solution for B_x is then completely determined for $x < 0$, as is the value of $\partial B_x/\partial x$ at $x = 0^-$. Similarly, the outer-region solution for $x > 0$, including the value of $\partial B_x/\partial x$ at $x = 0^+$, is completely determined from the boundary condition at $x \rightarrow \infty$ (or at an intervening conducting wall) and the requirement that it have the same amplitude, B_x , at $x = 0$ as has the solution for the left outer-region. It follows that the quantity Δ' is completely determined by the outer-region solutions. Indeed, later in this Chapter, we will calculate Δ' explicitly for our 'plasma current slab' configuration, but first we will analyze the resistive layer in more detail, to determine how it can provide the localized, concentrated currents j_z needed to produce the sharp 'jump' in B_{y1} and in $\partial B_x/\partial x$.

Problem 20.2: Show that the first-order 'surface current density' J_{z1} , i.e. the perturbed volume current density integrated in x across the resistive layer at any point y , is related to the value of B_x at this point y by $\mu_0 J_{z1} = i\Delta' B_x/k$. For the particular choice of phase in which $B_x = \bar{B}_x \sin(ky)$, show that $\mu_0 J_{z1} = (\Delta' \bar{B}_x/k) \cos(ky)$.

20.4 THE RESISTIVE LAYER

It is not sufficient merely to obtain 'boundary conditions' that apply across the resistive layer: it is necessary to resolve the fine-scale structure of this layer in order to determine the growth rate of the resistive tearing mode. Within the layer, we may certainly take $B_{y0} = B'_{y0}x$, and we may also make use of our finding that the perturbed field component B_x is approximately constant throughout the layer; this constant part of B_x will be denoted \bar{B}_x .

Equation (20.19) then becomes

$$\omega \bar{B}_x + k B'_{y0} x u_x = \frac{i\eta}{\mu_0} \frac{\partial^2 B_x}{\partial x^2} \quad (20.27)$$

where the term on the right-hand side evidently involves the non-constant part of B_x . Plasma inertia must also be included in the resistive layer, since we will see that the plasma flow velocities tend to peak in this region, implying that the full form of equation (20.12) must be used. However equation (20.12) may be simplified by noting that the x derivatives will tend to dominate over the y derivatives (i.e. the k -factors) in the thin resistive layer. Thus, an approximate form of equation (20.12) will suffice, namely

$$\begin{aligned} -\omega\rho_0\mu_0\frac{\partial^2 u_x}{\partial x^2} &= kB'_{y0}\frac{\partial}{\partial x}\left[x^2\frac{\partial}{\partial x}\left(\frac{B_x}{x}\right)\right] \\ &= kB'_{y0}\frac{\partial}{\partial x}\left(x\frac{\partial B_x}{\partial x} - B_x\right) \\ &= kB'_{y0}x\frac{\partial^2 B_x}{\partial x^2}. \end{aligned} \quad (20.28)$$

Substituting for $\partial^2 B_x/\partial x^2$ from equation (20.27), this becomes

$$\gamma\eta\rho_0\frac{\partial^2 u_x}{\partial x^2} = kB'_{y0}x(i\gamma\bar{B}_x + kB'_{y0}xu_x) \quad (20.29)$$

where we have also written $\omega = i\gamma$ in anticipation of finding the result that the tearing instability is purely growing.

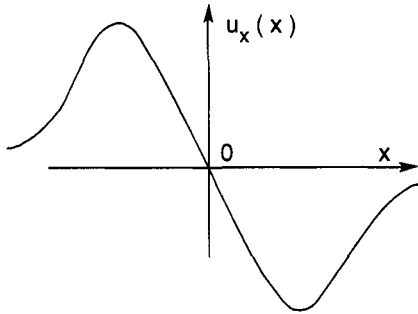


Figure 20.4. Typical form of the function $u_x(x)$ in the resistive layer.

Since \bar{B}_x is constant, equation (20.29) can be solved to find an explicit solution for the x dependence of u_x . Unfortunately, the solution cannot be given in terms of analytic functions but must be evaluated partially numerically. However, it is apparent from equation (20.29) that u_x will decrease steadily away from the resistive layer. Specifically, $u_x \sim -i\gamma\bar{B}_x/kB'_{y0}x \sim 1/x$ as $x \rightarrow \infty$ and the term on the left-hand side of equation (20.29) becomes negligible. It is also apparent that the solution u_x will be odd in x ; its actual

form is sketched in Figure 20.4. This implicitly assumes that the solution of the *inhomogeneous* equation (20.29) is *unique*, i.e. that the homogeneous equation obtained by omitting the term including $x\bar{B}_x$ has no permitted solutions. This latter result can be established easily, by multiplying the homogeneous equation by u_x^* and integrating from $-\infty$ to $+\infty$, thereby obtaining a negative-definite expression that must equal zero for any solution with $u_x \rightarrow 0$ as $x \rightarrow \infty$. The *characteristic width* of the resistive layer can be determined simply by inspection of equation (20.29). Balancing the term on the left-hand side against the second term on the right-hand side gives a characteristic width

$$x \sim \delta = (\gamma\eta\rho_0)^{1/4}/(kB'_{y0})^{1/2}. \tag{20.30}$$

As we might have expected, the resistive layer becomes thinner as the resistivity η decreases.

To complete the solution and find the growth rate γ , it is necessary to obtain an explicit solution of equation (20.29) in some form. For this purpose, it is convenient to transform to scaled variables X and U , which are defined by

$$\begin{aligned} X &\equiv x/\delta \\ U &\equiv (\gamma\eta\rho_0)^{1/4}(kB'_{y0})^{1/2}u_x/i\gamma\bar{B}_x. \end{aligned} \tag{20.31}$$

In terms of these variables, equation (20.29) becomes

$$\frac{\partial^2 U}{\partial X^2} = X(1 + XU). \tag{20.32}$$

The solution $U(X)$ will be an odd function of X and, as long as $\partial^2 U/\partial X^2$ is well-behaved as $X \rightarrow \pm\infty$, $U \rightarrow -X^{-1}$ as $X \rightarrow \pm\infty$. An explicit solution is obtainable in an integral form, namely

$$U(X) = -\frac{X}{2} \int_0^{\pi/2} \exp\left(-\frac{X^2}{2}\cos\theta\right) \sin^{1/2}\theta d\theta. \tag{20.33}$$

That this is the desired solution can be verified by direct substitution into equation (20.32), after first differentiating equation (20.33) twice to obtain

$$\frac{\partial^2 U}{\partial X^2} = \frac{X}{2} \int_0^{\pi/2} \exp\left(-\frac{X^2}{2}\cos\theta\right) \sin^{1/2}\theta(3\cos\theta - X^2\cos^2\theta)d\theta. \tag{20.34}$$

Using equations (20.33) and (20.34), we then obtain

$$\begin{aligned} \frac{\partial^2 U}{\partial X^2} - X^2U &= \frac{X}{2} \int_0^{\pi/2} \exp\left(-\frac{X^2}{2}\cos\theta\right) \sin^{1/2}\theta(3\cos\theta + X^2\sin^2\theta)d\theta \\ &= X \int_0^{\pi/2} \frac{d}{d\theta} \left[\sin^{3/2}\theta \exp\left(-\frac{X^2}{2}\cos\theta\right) \right] d\theta \\ &= X \end{aligned} \tag{20.35}$$

which establishes that equation (20.33) is indeed a solution of equation (20.32). Examination of the asymptotic form of equation (20.33) for large X , where the dominant contribution to the integral arises from values of θ near $\pi/2$, shows that equation (20.33) also has the correct asymptotic form, namely $U \rightarrow -X^{-1}$. This may be seen by changing the integration variable in equation (20.33) from θ to $\varphi = \pi/2 - \theta$, so that the asymptotic form for large X is obtained by approximating the integrand as $\exp(-X^2 \sin\varphi/2) \approx \exp(-X^2\varphi/2)$.

The purpose of analyzing the resistive layer in such detail is to obtain the correct boundary conditions to be applied to the solutions to the left and right of the resistive layer. We have seen in the previous Section that these outer-region solutions are completely defined when the surface current J_{z1} or, equivalently, the jump in B_{y1} or in $\partial B_x/\partial x$, is specified. From our equations for the resistive layer, the jump in $\partial B_x/\partial x$ can easily be obtained, for example by integrating equation (20.27) across the layer:

$$\left[\frac{\partial B_x}{\partial x} \right]_{x=0} = \frac{\mu_0}{i\eta} \int (i\gamma \bar{B}_x + k B'_{y0} x u_x) dx. \quad (20.36)$$

Reverting to our scaled variables X and U , and noting that the limits of integration in equation (20.36) may be taken as $\pm\infty$ on the scale of the resistive-layer width, i.e. the scale of X , we obtain

$$\frac{1}{\bar{B}_x} \left[\frac{\partial B_x}{\partial x} \right]_{x=0} = \frac{\gamma^{5/4} \rho_0^{1/4} \mu_0}{\eta^{3/4} (k B'_{y0})^{1/2}} \int_{-\infty}^{\infty} (1 + XU) dX. \quad (20.37)$$

The integral on the right-hand side of equation (20.37) can be evaluated numerically, using equation (20.33) for $U(X)$. It is also possible to reduce the integral to a particularly simple form using both equation (20.32) and its solution, equation (20.33). To do this, we proceed as follows:

$$\begin{aligned} \int_{-\infty}^{\infty} (1 + XU) dX &= \int_{-\infty}^{\infty} \frac{1}{X} \frac{\partial^2 U}{\partial X^2} dX \\ &= \frac{1}{2} \int_{-\infty}^{\infty} dX \int_0^{\pi/2} \exp(-\frac{1}{2} X^2 \cos\theta) \sin^{1/2}\theta (3\cos\theta - X^2 \cos^2\theta) d\theta \\ &= \frac{1}{2} \int_0^{\pi/2} \sin^{1/2}\theta d\theta \int_{-\infty}^{\infty} \exp(-\frac{1}{2} X^2 \cos\theta) (3\cos\theta - X^2 \cos^2\theta) dX \\ &= \left(\frac{\pi}{2}\right)^{1/2} \int_0^{\pi/2} \sin^{1/2}\theta (3\cos^{1/2}\theta - \cos^{1/2}\theta) d\theta \\ &= (2\pi)^{1/2} \int_0^{\pi/2} \sin^{1/2}\theta \cos^{1/2}\theta d\theta \approx 2.12 \end{aligned} \quad (20.38)$$

where the final integral in equation (20.38) has been evaluated numerically. The left-hand side of equation (20.37) is equated to the quantity Δ' which was

introduced in the previous Section and was defined in terms of the outer-region solutions. Equation (20.37) then gives an expression for the growth rate γ , namely

$$\gamma = 0.55 \Delta'^{4/5} \eta^{3/5} (k B'_{y0})^{2/5} / \rho_0^{1/5} \mu_0^{4/5}. \quad (20.39)$$

Once the quantity Δ' has been calculated from the properties of the outer solutions, equation (20.39) gives the growth rate of the resistive tearing instability.

Examination of equation (20.39) reveals some important information about the magnitude of the growth rate γ . In many cases of interest, it is appropriate to think of the resistivity η as a small quantity, i.e. the plasma obeys 'ideal magnetohydrodynamics' to a good approximation. The introduction of non-zero resistivity into the equilibrium will produce diffusion of plasma relative to the magnetic field, but only at a very slow rate, proportional to η . The introduction of non-zero resistivity into the stability calculation has, however, produced unstable modes that grow at a much faster rate, proportional to $\eta^{3/5}$.

This argument can be made more quantitative by defining various characteristic times. Let us first introduce a characteristic macroscopic length scale a , e.g. the half-width of the current slab shown in Figure 20.1. One characteristic time is the inverse of the frequency ω_A of a shear Alfvén wave with wave-number k propagating in the y direction, i.e. almost perpendicular to the assumed very strong magnetic field B_z . This shear Alfvén wave has $\omega = k_{\parallel} v_A = (k_y B_{y0} / B_z) v_A$; evaluating B_{y0} at the edge of the current slab, this time τ_A is defined by

$$\begin{aligned} \tau_A^{-1} = \omega_A &\approx (k_y B'_{y0} a / B_{z0}) v_A \\ &\approx k_y B'_{y0} a / (\rho_0 \mu_0)^{1/2}. \end{aligned} \quad (20.40)$$

A second characteristic time describes the diffusion of the field B_{y0} into the plasma due to non-zero resistivity; since the 'diffusion coefficient' for this process is η / μ_0 (see, for example, equation (20.18)), this time τ_R is defined by

$$\tau_R \approx a^2 \mu_0 / \eta. \quad (20.41)$$

Equation (20.39) may be rewritten in terms of τ_A and τ_R , giving

$$\gamma = \frac{0.55 (\Delta' a)^{4/5}}{\tau_A^{2/5} \tau_R^{3/5}}. \quad (20.42)$$

Equation (20.42) shows that resistive tearing instabilities grow on time-scales that are *intermediate* between the very short MHD time-scale, τ_A , and the very long resistive time-scale, τ_R . Indeed the relevant time-scale is close to the geometric mean of τ_A and τ_R . Thus, resistive tearing instabilities grow much

more slowly than ideal MHD instabilities (e.g. the flute instability, which has characteristic growth time $a/C_s \sim \beta^{-1/2}\tau_A$, i.e. approaching τ_A for finite β values), but much more rapidly than resistive diffusion of the equilibrium configuration. In this discussion, we have implicitly assumed that $\Delta'a$ is a quantity of order unity, which is generally valid, since Δ' is a characteristic of the macroscopic configuration. We will find that this assumption is confirmed, for example, in the case of the current slab analyzed in detail in the next Section.

20.5 THE OUTER MHD REGIONS

Until this point, we have not made use of any specific form for $B_{y0}(x)$ in the outer MHD regions, only that $B_{y0}(x) \approx B'_{y0}x$ in the narrow resistive layer around $x = 0$. Let us now find an explicit solution for the form of the perturbation in the outer-regions for the particular case of the plasma current slab illustrated in Figure 20.1 and specified in equations (20.1) and (20.2). To do this, we must solve equation (20.21) for the particular $B_{y0}(x)$ given in equation (20.2).

First consider the region $x > a$, where $B_y = B'_{y0}a = \text{constant}$. Here, equation (20.21) becomes simply

$$\frac{\partial^2 B_x}{\partial x^2} - k^2 B_x = 0 \quad (20.43)$$

whose only solution, vanishing as $x \rightarrow \infty$, is

$$B_x = C \exp(-kx) \quad (20.44)$$

where C is an arbitrary constant that measures the amplitude of the perturbation.

Next, consider the region $0 < x < a$, where $B_{y0} = B'_{y0}x$. Here, equation (20.21) takes the form

$$\frac{\partial}{\partial x} \left[x^2 \frac{\partial}{\partial x} \left(\frac{B_x}{x} \right) \right] - k^2 x B_x = 0 \quad (20.45)$$

but the derivative term can be expanded, i.e.

$$\begin{aligned} \frac{\partial}{\partial x} \left[x^2 \frac{\partial}{\partial x} \left(\frac{B_x}{x} \right) \right] &= \frac{\partial}{\partial x} \left(x \frac{\partial B_x}{\partial x} - B_x \right) \\ &= x \frac{\partial^2 B_x}{\partial x^2} \end{aligned} \quad (20.46)$$

so that equation (20.45) also becomes simply

$$\frac{\partial^2 B_x}{\partial x^2} - k^2 B_x = 0 \quad (20.47)$$

whose general solution is

$$B_x = A \exp(kx) + B \exp(-kx) \quad (20.48)$$

where A and B are arbitrary constants.

The solutions in the two regions must be matched at $x = a$. The correct matching conditions are obtained from equation (20.21), which applies throughout the outer region, including both $x < a$ and $x > a$, and they are

$$\begin{aligned} B_x|_{x=a-} &= B_x|_{x=a+} \\ \frac{\partial}{\partial x} \left(\frac{B_x}{B_{y0}} \right) \Big|_{x=a-} &= \frac{\partial}{\partial x} \left(\frac{B_x}{B_{y0}} \right) \Big|_{x=a+} \end{aligned} \quad (20.49)$$

the latter following from integrating equation (20.21) across an infinitesimal boundary layer at $x = a$. For the solutions given in equations (20.44) and (20.48), the two conditions expressed in equation (20.49) give

$$\begin{aligned} A \exp(ka) + B \exp(-ka) &= C \exp(-ka) \\ A(ka - 1) \exp(ka) - B(ka + 1) \exp(-ka) &= -Cka \exp(-ka). \end{aligned} \quad (20.50)$$

From these relations, the constants A and B can easily be obtained in terms of C :

$$A = \frac{C}{2ka} \exp(-2ka) \quad B = \frac{C}{2ka} (2ka - 1). \quad (20.51)$$

This completes the solution for $x > 0$. One arbitrary constant, in this case C , must remain, since the amplitude of a perturbation in linear theory is indeterminate.

Since the form of the equilibrium to the left of $x = 0$ is exactly the same as that to the right of $x = 0$, the solution for $x < 0$ can be obtained by simply substituting $-x$ for x in the solution which we have already found. Specifically, for $-a < x < 0$, the solution is

$$B_x = A \exp(-kx) + B \exp(kx) \quad (20.52)$$

and, for $x < -a$, it is

$$B_x = C \exp(kx) \quad (20.53)$$

with the same values of the constants A , B and C .

It is now possible to calculate the quantity Δ' defined in equation (20.26). Specifically,

$$\Delta' \equiv \frac{1}{B_x} \left[\frac{\partial B_x}{\partial x} \right]_{x=0} = \frac{2k(A - B)}{A + B}. \quad (20.54)$$

Substituting for A and B in terms of C using equation (20.51), we obtain

$$\Delta'a = \frac{2ka[\exp(-2ka) - 2ka + 1]}{\exp(-2ka) + 2ka - 1}. \quad (20.55)$$

In Figure 20.5, we plot the function $\Delta'a$ versus ka . We see that Δ' is positive for small k (long wavelengths in the y direction) and negative for large k (short wavelengths in the y direction).

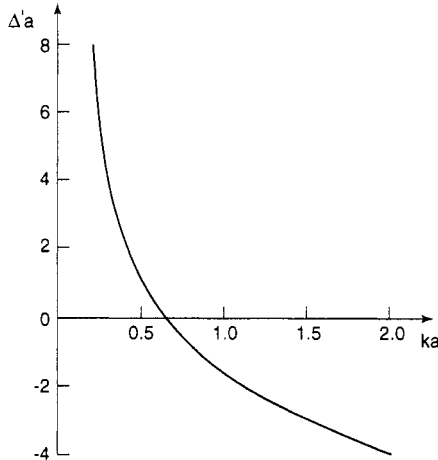


Figure 20.5. The function $\Delta'a$ describing tearing-mode stability plotted against ka .

Since $\Delta' > 0$ is the condition for the resistive tearing mode to be unstable, we have now shown that the 'plasma current slab' equilibrium is, in fact, unstable to all perturbations that are wave-like in the y direction and have sufficiently long wavelength.

As we saw at the beginning of this Chapter, the annihilation of magnetic field, by means of the cancellation of positive and negative B_y components in a small region $|x| < \delta$, is energetically favored, i.e. it lowers the magnetic energy. However, as we have now seen, a magnetic perturbation that is wave-like in the y direction is required to produce the B_x component at $x = 0$ needed for the negative B_y field to connect to, and thereby annihilate, the positive B_y field. This wave-like perturbation necessarily involves bending of the field lines, which requires energy in an amount that increases as the wavelength decreases. Thus it should not be surprising that the resistive tearing mode is unstable only for sufficiently long wavelengths, i.e. wavelengths for which the energy released by field annihilation exceeds that needed for field bending.

We also saw earlier in this Chapter that a general sheared-field plasma slab configuration with both $B_y(x)$ and $B_z(x)$ could be susceptible to resistive tearing

instabilities at many locations x , depending on which modes of perturbation are allowed by the boundary conditions. This has an important application to the 'cylindrical tokamak', which is a model configuration with a strong, approximately uniform axial field B_z and a weaker azimuthal field $B_\theta(r)$. The normal modes of perturbation of an infinitely long cylindrical plasma are of the form $\exp(im\theta + ik_z z)$, where m must be an integer but k_z can have any value. However, in the tokamak case, the cylinder is an approximation to a 'straightened out' torus and should therefore be considered to have finite length $2\pi R$, where R is the major (larger) radius of the torus. Moreover, 'periodic boundary conditions' should be applied at the ends of the now-finite-length cylinder, so that we must take $k_z = -n/R$ where n is an integer (the choice of a negative sign being simply for convenience, as we will soon see, since both positive and negative integers are allowed). Such a perturbation can be 'resonant', in the sense that $\mathbf{k} \cdot \mathbf{B} \equiv mB_\theta/r - nB_z/R$ will vanish at a radius r where $q(r) \equiv rB_z/[RB_\theta(r)] = m/n$. This is the equivalent of the resonant surface in our 'slab' calculation at $x = 0$, where $\mathbf{k} \cdot \mathbf{B} \equiv k_y B_{y0} = 0$. For a tokamak with a current distribution $j_z(r)$ that peaks at $r = 0$ and decreases to zero at the plasma edge, $r = a$, the function $q(r)$ will increase monotonically from a minimum value at $r = 0$ to a maximum value at $r = a$. Clearly, infinitely many rational numbers m/n can be 'fitted in' between $q(0)$ and $q(a)$. However, since we have seen that only large wavelengths tend to be unstable to resistive tearing modes, only 'low-order' rationals, i.e. those for which m and n are small integers, are of interest. By far the most unstable mode in a tokamak is that with $m = n = 1$, and the nonlinear evolution of this mode tends to strongly flatten the plasma profiles inside of the resonant surface; however, this mode can arise only when $q(0) < 1$. The mode with $m = 2, n = 1$ is also dangerous, since it can occur whenever $q(0) \approx 1$ and $q(a) > 2$. However, the stability of any particular mode is determined not just by the presence of the associated resonant surface, but also by the form of the plasma current distribution; in many cases, all modes can be stable.

Problem 20.3 Suppose that rigid conducting walls are introduced into our plasma current slab at $x = \pm b$ (with $b > a$). Find the generalization of equation (20.55) for $\Delta'a$ in this case. Do you expect the plasma to be more, or less, stable? Is this expectation confirmed by your expression for $\Delta'a$?

20.6 MAGNETIC ISLANDS

The resistive tearing instability produces a change in the topology of the magnetic field. The magnetic configuration of the plasma current slab before onset of the

instability is illustrated in Figure 20.2. The field lines are straight and, assuming that a strong approximately uniform B_z component is added to the B_y component shown in Figure 20.2, lie in flat surfaces parallel to the (y, z) plane. The direction of the B_y component reverses across $x = 0$. After onset of the instability, the magnetic configuration is deformed, and the field lines now lie on modified surfaces, which are still uniform in the z direction (since there is no variation of the perturbation in the z direction) but which intersect the (x, y) plane in curved lines determined by the relations $dx/dl = B_x/B$ and $dy/dl = B_y/B$. In effect, all of the deformed field lines project in the z direction onto the (x, y) plane to curved lines given by

$$\frac{dx}{dy} = \frac{B_x}{B_y}. \quad (20.56)$$

In essence, the configuration illustrated in Figure 20.2 is modified to that given by the solution of equation (20.56).

For small-amplitude perturbations, the B_y component can be approximated by its equilibrium value, $B_y \sim B'_{y0}x$. For a particular choice of phase (in order to deal with real quantities, rather than complex ones such as $\exp(iky)$), the B_x component at some particular time t can be written

$$B_x = \bar{B}_x e^{\gamma t} \sin(ky) \quad (20.57)$$

where, as we have seen, the quantity \bar{B}_x can be taken as approximately independent of x within the resistive layer around $x = 0$. Equation (20.56) can then be integrated to give

$$\frac{1}{2} B'_{y0} x^2 + \frac{\bar{B}_x}{k} e^{\gamma t} \cos(ky) = \text{constant} \quad (20.58)$$

where different values of the constant give the projections of different field lines onto the (x, y) plane.

The solutions of equation (20.58) can easily be plotted in the (x, y) plane, and a typical example is illustrated in Figure 20.6. At relatively large values of $|x|$, corresponding to large values of the constant in equation (20.58), the field lines are only slightly distorted from the unperturbed configuration shown in Figure 20.2. However, the distortion increases for smaller values of $|x|$, corresponding to smaller values of the constant in equation (20.58), and eventually the field lines become 'closed on themselves'. Inspection of equation (20.58) shows that these 'closed' field lines arise from values of the constant less than $(\bar{B}_x/k) \exp(\gamma t)$, for which only a limited range of y values are possible, since for these values of the constant equation (20.58) does not allow $\cos(ky)$ to reach unity for any real value of x .

The closed field line regions shown in Figure 20.6 are called 'magnetic islands'. When the strong approximately uniform B_z field is taken into account,

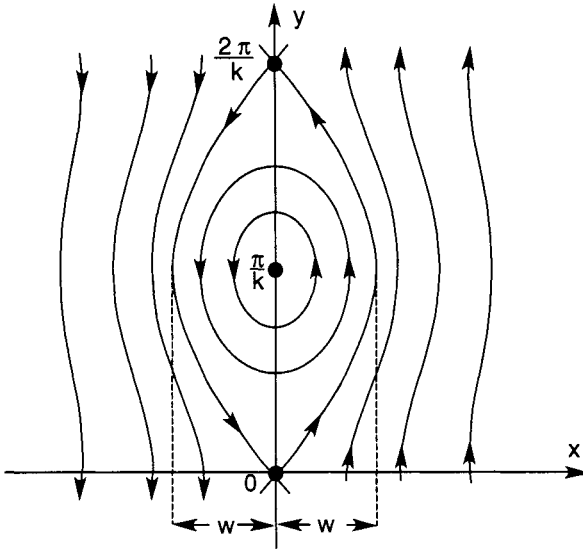


Figure 20.6. Perturbed field line configuration of magnetic islands of half-width w produced by a resistive tearing instability. The pattern is repeated with period $2\pi/k$ in the y direction.

the individual field lines will not actually close on themselves, but will traverse surfaces whose shapes will approximate elliptical cylinders, which are infinitely long in the z direction. In this case, Figure 20.6 depicts the intersections of these surfaces with the (x, y) plane at $z = 0$ or, equivalently, the projection of the field lines onto this plane. A given field line will always remain on the same surface, and its projection onto the (x, y) plane at $z = 0$ will traverse the closed curves shown in Figure 20.6 over and over again as it proceeds further and further in the z direction.

The surface that separates the closed field line surfaces from the open field line surfaces is usually called the 'magnetic separatrix'. The separatrix corresponds to a value of the constant in equation (20.58) exactly equal to $(\bar{B}_x/k)\exp(\gamma t)$. The half-width w of the magnetic island formed by the separatrix, which is of course the largest magnetic island (see Figure 20.6), is simply the value of x given by equation (20.58) for this value of the constant and at $ky = \pi$, namely

$$w = 2(\bar{B}_x/kB'_{y0})^{1/2}\exp(\gamma t/2). \quad (20.59)$$

The half-width of the magnetic island is proportional to the square-root of the field perturbation \bar{B}_x , so it increases exponentially in time, as indicated in equation (20.59). In practice, nonlinear effects will limit the growth of magnetic

islands when significant modifications are produced in the underlying magnetic configuration on which our stability analysis was based. Such effects begin to appear as soon as the island width becomes comparable to the width of the resistive layer given by equation (20.30), as was shown in a paper by one of the authors of this present book (P H Rutherford 1973 *Phys. Fluids* **16** 1903). When the island grows to a significant fraction of the size of the overall configuration, it can affect the gross current profile, usually acting to reduce the value of $\Delta'a$ and thereby tending to stabilize the tearing mode.

There is clearly a close connection between the magnetic islands and magnetic separatrix obtained here and the islands and separatrices found in the numerical analysis of area-preserving maps presented in connection with particle orbits in Chapter 5. Indeed, the field line equation of motion, equation (20.56), can be represented as a map, where a point is laid down each time a distance $2\pi R$ is traversed in the z direction. The shear in the magnetic field is then equivalent to the sheared particle flow for the problem in Chapter 5, and many of the previous results carry through. The island width at the rational surface, for example, scales in both cases with the square-root of the perturbation strength. Were we to attempt a numerical treatment of the effects of resistive tearing instabilities, we would expect to find, at least in some cases, not only a primary island chain, but also secondary chains of smaller islands, as in Figure 5.2. When the mode amplitude grows so large that secondary islands begin to overlap with the primary island or, in cases where several different modes are unstable, primary island chains begin to overlap with each other, then the magnetic field structure becomes 'stochastic'. When this occurs, an individual field line can find its way completely across the plasma (i.e. in the x direction for the plasma slab configuration considered in this Chapter), if followed a sufficient distance. As a practical consequence, this will generally mean that electron thermal conduction parallel to the magnetic field will rapidly flatten the electron temperature across the stochastic region.

The origin of the name 'tearing mode' is now apparent. The magnetic configuration illustrated in Figure 20.2 'tears' at its weakest points, i.e. along the plane $x = 0$. Provided the conditions for instability are satisfied (i.e. positive Δ'), the plasma current slab will then have a tendency to break up into discrete current 'filaments'.

Problem 20.4 The result of Problem 20.2 implies that the first-order perturbed current density in the z direction is *negative* at the 0-point of the magnetic island, i.e. the point $(0, \pi/k)$ in Figure 20.6, for an unstable mode ($\Delta' > 0$), and *positive* at the X-point of the island, i.e. the point $(0,0)$ in Figure 20.6. (It should be noted that this is a special property of our choice of geometry; the signs are reversed, for example, in a cylindrical

tokamak configuration with $dq/dr > 0$.) Verify this for the slab geometry by a different method, as follows. Consider the magnetic flux 'trapped' within the magnetic island. Referring to Figure 20.6, we may view this flux as that of the B_x field crossing the y axis between the X-point and the O-point; per unit length in the z direction, this flux is

$$\Psi = \int_0^{\pi/k} B_x(0, y) dy.$$

By employing the usual combination of Faraday's law and Ohm's law, show that

$$\frac{d\Psi}{dt} = \eta [j_z(0, 0) - j_z(0, \pi/k)]$$

(Hint: Note that the magnetic field is *exactly* in the z direction at both the O-point and the X-point, which precludes convection of flux across the boundaries of the surface under consideration.) The trapped flux Ψ must increase as the instability and island-width grow. What does this tell us about the magnitude of the perturbed current density j_z at the island O-point, versus that at the X-point?